

## Plasma flow injection into a torus chamber as a new approach to flowing two-fluid plasma generation

M. Nagata<sup>1</sup>, T. Takamiya<sup>1</sup>, T. Kanki<sup>2</sup>, Y. Onishi<sup>1</sup>, N. Fukumoto<sup>1</sup> and S. Masamune<sup>3</sup>

<sup>1</sup> *University of Hyogo, Himeji, Japan*

<sup>2</sup> *Japan Coast Guard Academy, Kure, Japan*

<sup>3</sup> *Kyoto Institute of Technology, Kyoto, Japan*

### I. Introduction

The importance of plasma flow or two-fluid effect is recognized in understanding the relaxed states of high-beta torus plasmas, current drive by coaxial helicity injection, magnetic reconnection and plasma dynamo in fusion, laboratory and space plasmas [1]. A more general relaxation theory was developed based on the two-fluid model, showing that a finite beta plasmas appears in relaxed states with flow [2]. Equilibrium calculations based on a two-fluid model in the helicity driven system predicted that there exists a diamagnetic low safety factor  $q$  spherical torus (ST) with higher beta [3]. For the purpose of studying the general relaxation of flowing two-fluid plasmas, we have tried to inject tangentially the magnetized plasma flow with spheromak-type magnetic field structures, i.e., compact torus (CT) plasma flow, into a torus vacuum chamber. During the injection process, we expected that the plasma flow relaxes towards the reversed-field pinch (RFP)-like states characterized by finite pressure and significant poloidal and toroidal sheared flows. This paper presents formation of RFP-like relaxed plasmas by CT flow injection and a major role of ion flow in the relaxation during the formation.

### II. Experimental setup

Figure 1 shows schematics of the experimental device, indicating the magnetized coaxial plasma gun (MCPG), a straight drift tube, a torus vacuum chamber ( $R/a = 0.25$  m/0.083 m) with the toroidal magnetic field (TF) coils and diagnostics. The CT plasma flow is produced by a single stage MCPG. The MCPG is  $\sim 1.0$  m long, with inner and outer electrode diameters 0.06 m and 0.14 m, respectively. This is operated with capacitor banks (30 kJ, 10 kV). The peak gun current  $I_{g,max}$  is about 60 kA and its half cycle is 150  $\mu$ s. The outer bias solenoid coil wound on the outer electrode produces the bias flux  $\Psi_{bias}$

of 3 - 4 mWb. The ion flow velocity  $u_i$ , electric field  $E$  and electron density  $n_e$  are measured by a directional Mach probe on which two double probes are mounted.

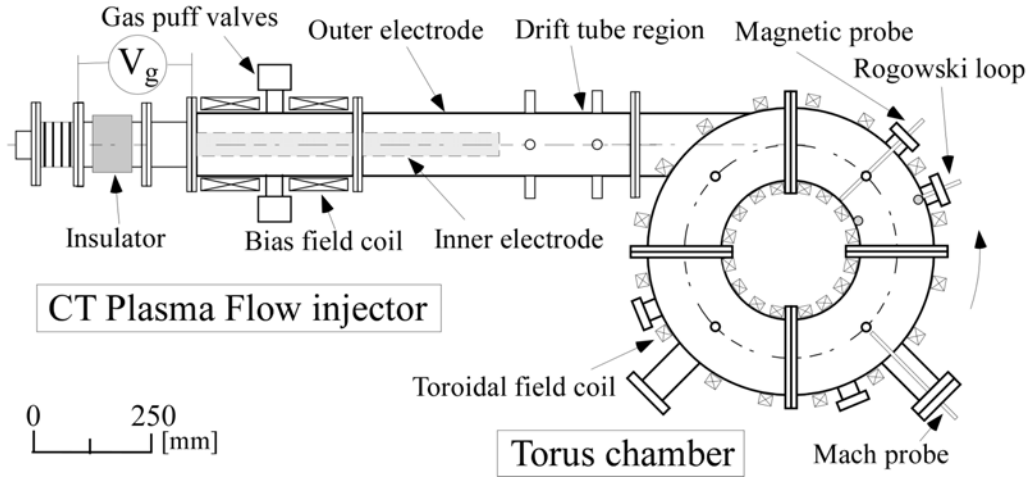


Figure 1. Schematics of the experimental device and diagnostics for CT plasma flow injection into the torus vacuum chamber with the toroidal field coil.

### III. Experimental results

#### A. Performance of the CT flow as a function of the gun bank voltage

Figure 2 (a) shows the toroidal current  $I_t$  and the axial ion flow velocity  $u_{i,z}$  as a function of the gun capacitor bank voltage  $E_g$ . The toroidal current driven in the torus chamber by the plasma injection is measured by Rogowski loops. Figure 2 (b) shows the electron density  $n_e$  as a function of  $E_g$ . As increasing  $E_g$ , the axial ion flow velocity, the electron density and the toroidal current increase, and for  $E_g = 7$  kV, each value of  $u_{i,z}$ ,  $n_e$ , and  $I_t$  is 27 km/s,  $8 \times 10^{19} \text{ m}^{-3}$  and 20 kA, respectively. The time duration of the flow injection is  $\sim 60 \mu\text{s}$ . The CT flow propagating in the drift tube has helical magnetic field structures.

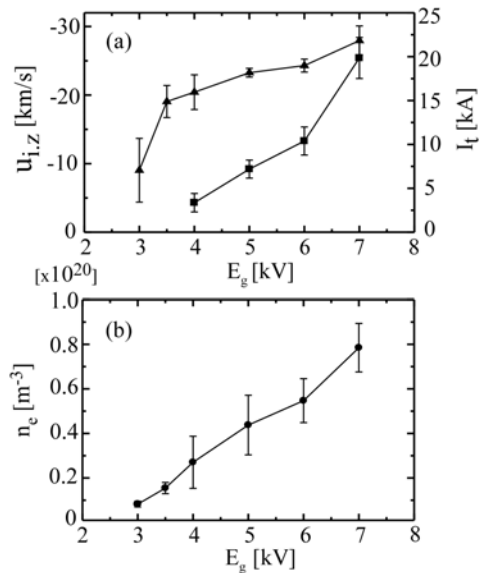


Figure 2. (a) Ion flow velocity  $u_{i,z}$  along the axial direction and toroidal current  $I_t$  versus the charging voltage  $E_g$  of gun capacitor banks. (b) Electron density  $n_e$  versus  $E_g$ .

### B. Performance of toroidal plasmas produced in the torus as varying the TF

The dependences of the  $I_t$  generation and internal magnetic field profiles in the confinement chamber upon the strength and direction of the TF have been examined. Figure 3 displays  $I_t$  versus  $\Psi_{TF}$ . Reversing the direction of the TF, we have interestingly found that the sign of the toroidal current is reversed. The direction of  $I_t$  without TF is determined by that of only the gun current. Figure 4 shows the radial profiles of the three magnetic field components ( $B_r$ ,  $B_\theta$ ,  $B_z$ ) and the vacuum field  $B_{vac,z}$  in three cases ( $\Psi_{TF}=0$ ,  $\Psi_{TF}>0$ ,  $\Psi_{TF}<0$ ). It has been found that the RFP-like configuration with helical component ( $m = 0$  and  $m = 1$  mixed state [4]) is formed in the case of  $\Psi_{TF}=0$  (see the reversal of the edge toroidal field  $B_z$ ). Applying the TF reduces effectively the amplitude of  $B_r$ . For  $\Psi_{TF}<0$ , we can see that not only the toroidal field  $B_z$  but also the poloidal field  $B_\theta$  reverses its sign in comparison with that of  $\Psi_{TF}=0$  and  $\Psi_{TF}>0$ . When we reversed the polarity of the bias flux of the gun, the direction of the toroidal current was reversed in both  $\Psi_{TF}>0$  and  $\Psi_{TF}<0$ . This result suggests that the magnetic helicity  $K$  is conserved during the injection.

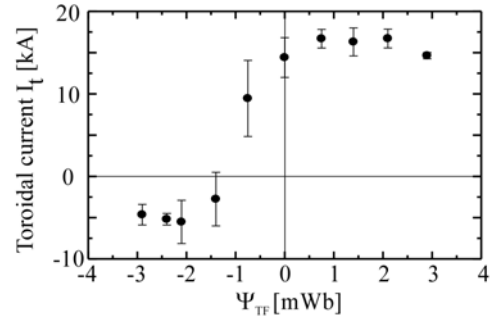


Figure 3. Toroidal current  $I_t$  measured in the torus chamber region versus the external toroidal flux  $\Psi_{TF}$ .

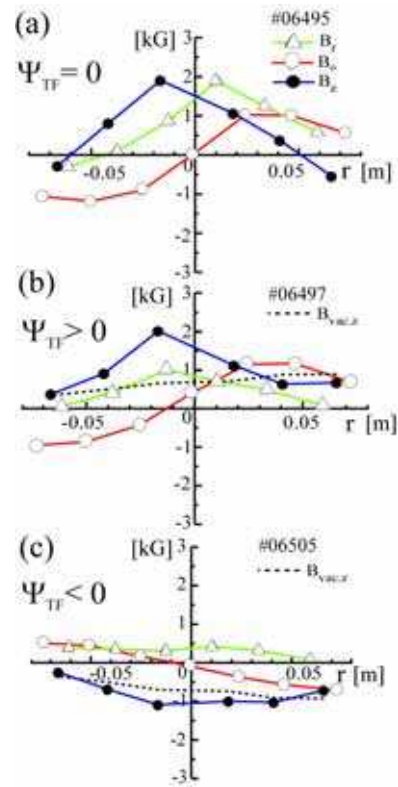


Figure 4. Radial profiles of magnetic fields measured on the midplane in the torus chamber for each case ( $\Psi_{TF}=0$ ,  $\Psi_{TF}>0$ ,  $\Psi_{TF}<0$ ).

### C. Contribution of the ion flow to the toroidal current

Figure 5 shows the dependence of the ion flow velocity  $u_i$  on the variation of the TF. It should be noted that the direction of the ion flow was not changed for  $\Psi_{TF}<0$

despite the reversal of  $I_t$ . Thus, this result suggests that the ion flow has a significant contribution to the toroidal current in the torus. The electron flow velocity  $u_{e,z}$  can be inferred from the measured current density  $J_z$  which is expressed by  $J \sim en(u_i - u_e)$ , where density  $n \sim n_e$ . For  $\Psi_{TF} > 0$ ,  $u_{e,z} \sim -124$  km/s and  $u_{i,z} \sim -35$  km/s, but in this case, the ion flow has no contribution to  $I_t = 10$  kA. In the other hand, for  $\Psi_{TF} < 0$ , we obtained  $u_{e,z} \sim 45$  km/s and  $u_{i,z} \sim -20$  km/s, and so  $u_{i,z}$  plays an significant role in the current drive in the opposite direction of  $I_t = -2.5$  kA.

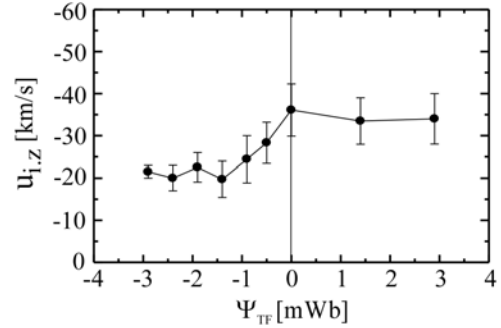


Figure 5. Ion flow velocity  $u_{i,z}$  in the axial direction versus the toroidal flux  $\Psi_{TF}$ . The direction of the ion flow is same between  $\Psi_{TF} > 0$  and  $\Psi_{TF} < 0$ .

#### IV. Discussions and conclusions

As reversing the direction of the TF, the toroidal plasma current also was reversed. However, the ion flow measurement showed that the ion flow keeps the same direction despite the reversal of the toroidal current and the axial electric field. The ion fluid comes to flow in the opposite direction to the electron fluid by the reversal of TF. This result suggests that not only electron but also ion flow contributes significantly on the reversed toroidal current. In this case, the ratio of  $u_i$  to  $u_e$  was estimated as  $u_i/u_e \sim 1/2$ . At the present experiment, the generation of a perpendicular current due to the ion diamagnetic drift has not been observed satisfactorily although the role of the ion flow in the driven current has emerged by the TF reversal. The ratio of this system size scale to the ion skin depth,  $S^* < 6$  is relatively smaller as compared to large ST/CT devices, so the two-fluid effect should become more important.

The authors are grateful to Drs. L.C. Steinhauer and A. Ishida for useful discussions and suggestions.

#### References

- [1] H. Y. Guo et al, Phys Rev. Lett. 92, 245001-1 (2004)
- [2] L. C. Steinhauer and A. Ishida, Phys. Rev. Lett. 79, 3423 (1997), S. M. Mahajan and Z. Yoshida, Phys. Rev. Lett. 81, 4863 (1998)
- [3] T. Kanki, M. Nagata and T. Uyama, Proc. of 30th European Physical Society Conference on Controlled Fusion and Plasma Physics, July 7-11, 2003, St Petersburg, ECA Vol. 27A, CD-ROM file P-3.217.
- [4] J. B. Taylor, Reviews of Modern Physics 58, 741 (1986)